SEMI ANNUAL STATUS REPORT

TO THE

NATIONAL AERONAUTICS AND SPACE ADMINISTRATION

ON

RUBIDIUM^{87} GAS CELL STUDIES

(PHASE II)

NGR 52-133-001

Period covered: August 1, 1972 to March 1, 1973

Quantum Electronics Laboratory
Department of Electrical Engineering
Laval University
Quebec, Canada
G1K 7P4

March 1973

SEMI ANNUAL STATUS REPORT

TO THE

NATIONAL AERONAUTICS AND SPACE ADMINISTRATION

ON

RUBIDIUM^{87} GAS CELL STUDIES

(PHASE II)

NGR 52-133-001

Period covered: August 1, 1972 to March 1, 1973

Quantum Electronics Laboratory
Department of Electrical Engineering
Laval University
Quebec, Canada
G1K 7P4

March 1973

FOREWORD

This is a semi-annual status report relative to the construction of a compact Rubidium^{87} maser and its associated electronics, work carried out in the Quantum Electronics Laboratory of Laval University. The work is considered to be the second phase of a program design to develop rubidium masers.

Along with this development, some basic work on the rubidium maser is carried out on a continuous basis in the laboratory. This last type of work is sponsored by other agencies such as the National Research Council of Canada and is reported briefly here. Also attached as annexes are one paper which has been submitted for publication and an abstract of a paper which will be given at the 27th Annual Frequency Control Symposium in June 1973.

Jacques VANIER
Professor
(Principal investigator)

INTRODUCTION

The project consists in the development of three systems:

a) A compact rubidium^{87} maser

b) An electronic control system for the maser itself

c) A superheterodyne receiver capable of locking a crystal oscillator to the maser signal.

These are the three major tasks that were proposed in our proposal QE4 entitled "Rb^{87} Gas Cells Studies" phase II.

Our plans have not been changed and we are in the process of accomplishing these three tasks.

The present report is short and describes as concisely as possible the state of construction of the maser. It may not give all the details of the design of the maser and of the electronics associated with the masers. However, complete details will be given in the final report of this project.

STATUS OF THE WORK

The present status of our work can be summarized as follows :

a) The Rubidium^{87} Maser

The schematic diagram of the maser we were planning to construct and which was shown in our proposal has been somewhat altered. A diagram of the new design is shown in Figure 1. We kept the original design as

close as possible as far as general layout of parts and size are concerned. Actually, the only major change has been the introduction of a main aluminium cylinder serving as a support for various parts thus eliminating the necessity of the holding rods. The maser consists of a main manifold attached to a base and serving as a support for the whole system. The quartz cavity, the copper cavity bottom plate and the transparent top plates are attached to this cylinder. The top plunger of the cavity is transparent to light and is held in mechanical contact with the cavity cylinder by beryllium copper springs. The arrangement provides a certain amount of compensation against temperature fluctuations. The temperature of the cavity is maintained at the desired value by heaters wound on the main cylinder. This temperature should be of the order of $60^{o}C$. The filter cell is attached to the main cylinder through an aluminium ring. The temperature of the filter cell is controlled independently of the main cylinder. The attachment ring, however, provides a cold spot which serves as rubidium reservoir and prevents condensation of rubidium on the face of the filter. The filter attachment is made versatile enough to accomodate various sizes of filter cells. The lamps itself is attached to the main cylinder and consists of seven small cells driven individually by separate oscillators. We expect to regulate its temperature with a single control. The whole system is placed inside three magnetic shields made of moly permalloy.

At the present date, we may report the following :

i) The detailed design of all parts has been completed. The maser will be 35cm long by 25cm in diameter. The magnetic shields have been received from the manufacturor and also the

quartz cavity and the quartz bulb. In all, approximately 60% of the maser parts have been fabricated.

ii) The mechanical parts of the multiple-cell lamp have been constructed. A breadborad of the oscillators for exciting the lamp has been constructed and seems to operate well. Four lamps in the multiple cells arrangement have been operated simultaneously. We will add the three other lamps upon receiving the special condensors required for this operation. The lamp is probably one of the most critical parts of the maser and its final assembly will require extra care to keep the equilibrium temperature of the various sections.

b) Maser Electronics Control

The maser electronics consist essentially of approximately six (6) thermal control assemblies and one magnetic field control assembly. Construction of these items has been started. They represent standard items in our laboratory and they can be fabricated under short notice.

c) Super Heterodyne Receiver

The receiver on which our choice was made is shown in Figure 2. It is slightly different from the one shown in our proposal. The system is being constructed with modules. All the items that are available commercially at a moderate price have been ordered and many of them were received. Two modules create a slight difficulty :

1. The frequency multiplier (X68) is not available commercially. It is being constructed in our laboratory.

2. Our choice has not yet been made for the frequency synthesizer. We may have to build one if it is not available commercially at a moderate price.

CONCLUSION

Our work is progressing normally. The maser and the electronic systems are completely designed and the construction is well underway. We scheduled to complete the whole system approximately by the month of August 1973. It appears that this is still feasible although we may have to concentrate special efforts on such items as the X68 frequency multiplier and the synthesizer.

FIGURE CAPTIONS

Figure 1 : Compact rubidium^{87} maser design

Figure 2 : Superheterodyne receiver for the maser signal detection

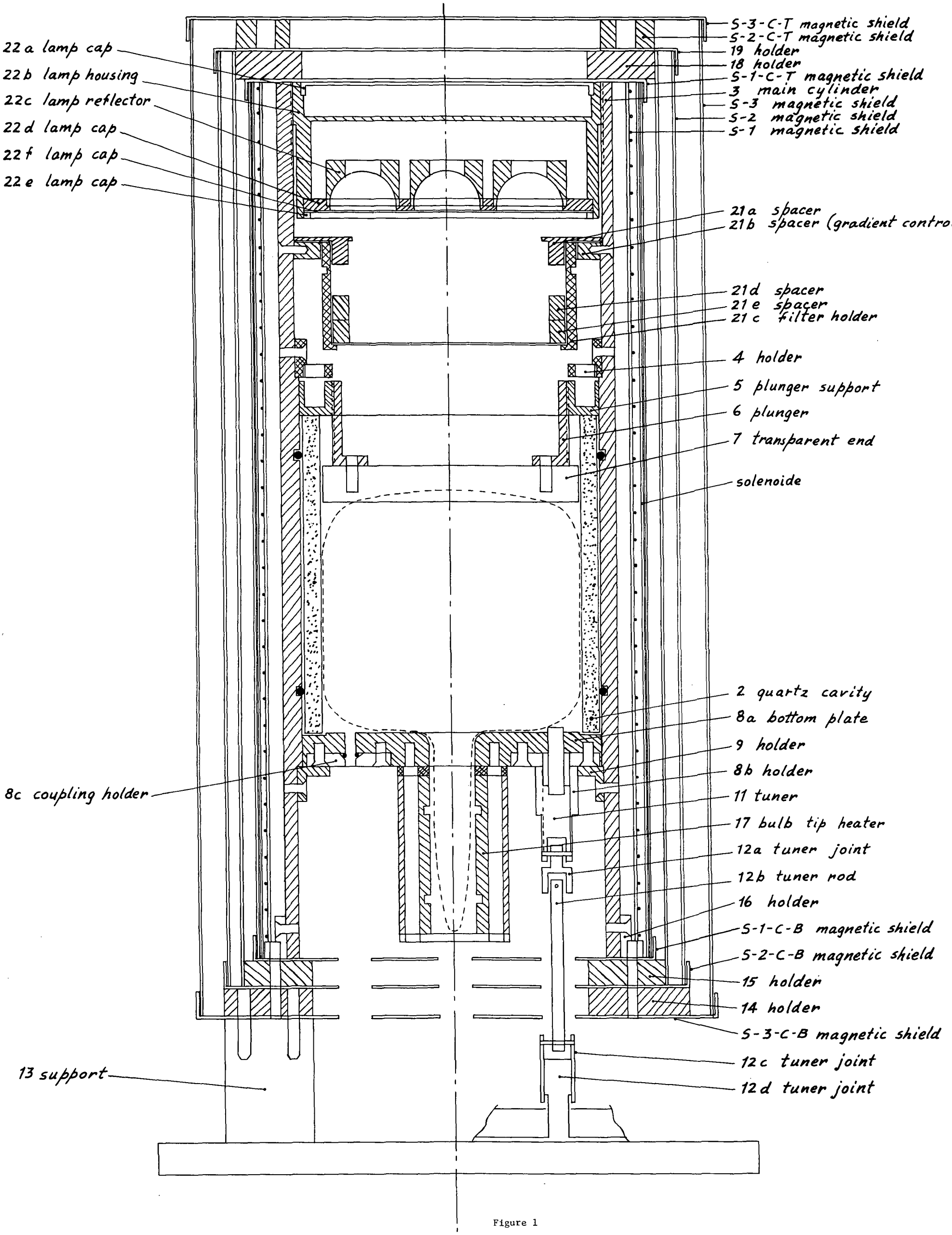
22 a lamp cap
22 b lamp housing
22c lamp reflector
22 d lamp cap
22 f lamp cap
22 e lamp cap
S-3-C-T magnetic shield
S-2-C-T magnetic shield
19 holder
18 holder
S-1-C-T magnetic shield
3 main cylinder
S-3 magnetic shield
S-2 magnetic shield
S-1 magnetic shield
21a spacer
21b spacer (gradient control)
21d spacer
21 e spacer
21 c filter holder
4 holder
5 plunger support
6 plunger
7 transparent end
solenoide
2 quartz cavity
8a bottom plate
9 holder
8b holder
11 tuner
17 bulb tip heater
12a tuner joint
12b tuner rod
16 holder
S-1-C-B magnetic shield
S-2-C-B magnetic shield
15 holder
14 holder
S-3-C-B magnetic shield
12c tuner joint
12d tuner joint
8c coupling holder
13 support

Figure 1

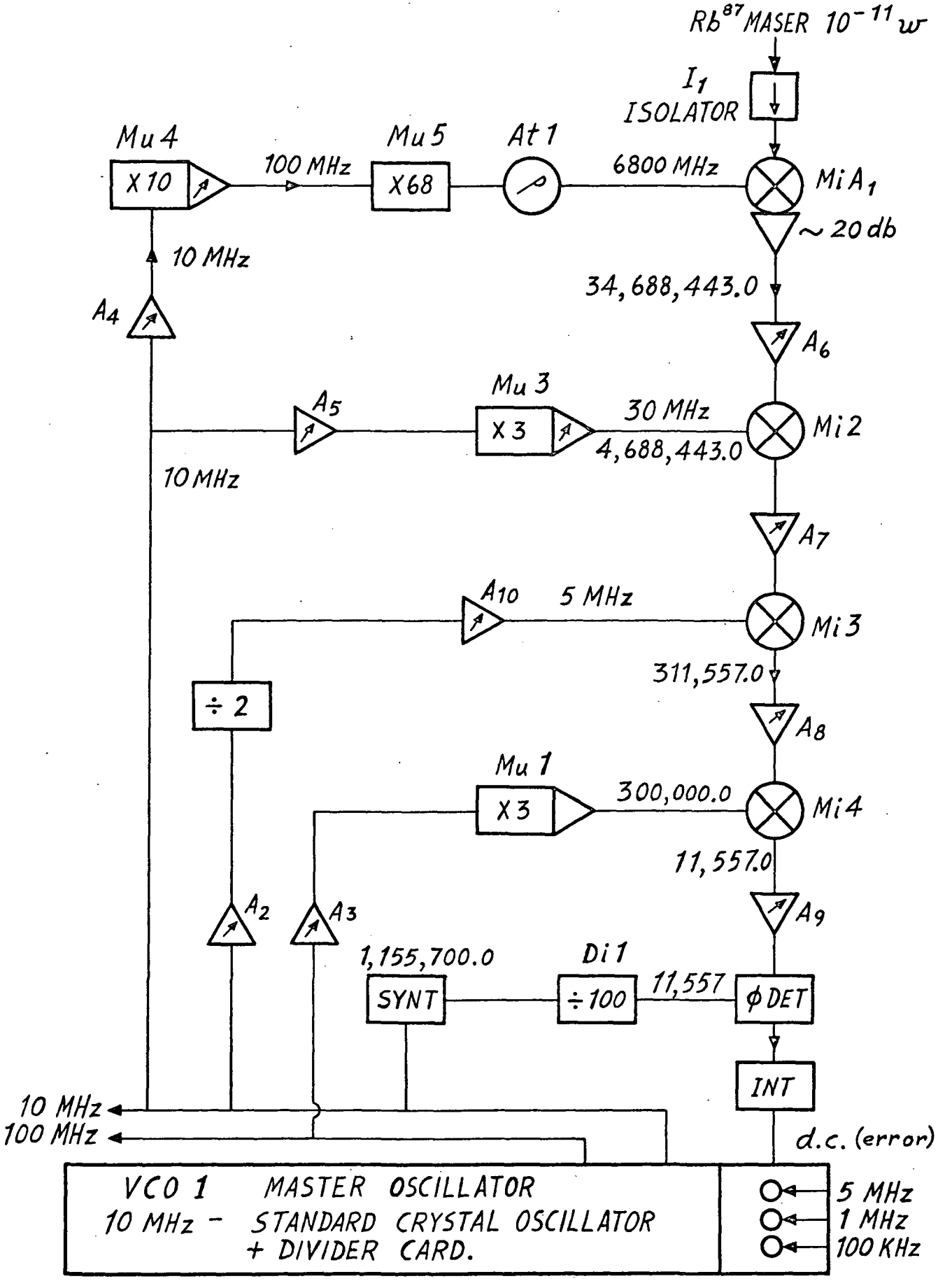
Rb87 MASER 10-11 w
I1
ISOLATOR
Mu 4
X 10
100 MHz
Mu 5
X 68
At 1
6800 MHz
Mi A1
~ 20 db
10 MHz
34,688,443.0
A4
A6
Mu 3
A5
X 3
30 MHz
4,688,443.0
Mi 2
10 MHz
A7
A10
5 MHz
Mi 3
311,557.0
÷ 2
A8
Mu 1
X 3
300,000.0
Mi 4
11,557.0
A2
A3
A9
1,155,700.0
Di 1
SYNT
÷ 100
11,557
φ DET
INT
10 MHz
100 MHz
d.c. (error)
VCO 1 MASTER OSCILLATOR
10 MHz - STANDARD CRYSTAL OSCILLATOR
+ DIVIDER CARD.
5 MHz
1 MHz
100 KHz

Figure 2

ANNEX A

Along with these developments we may report some work of a more fundamental nature being conducted in the laboratory.

1) Vacuum tight cavity maser : This project is being conducted
   a) in order to verify the possibility of obtaining more power out of a rubidium maser through a higher Q cavity
   b) in order to make experiments on a maser operating with a mixture of buffer gases giving a nearly zero temperature coefficient.

2) Other experiments are being conducted on the two "quartz cavity - quartz bulb" type masers. These experiments are of two types. One consists in looking for the possibility of tuning the maser cavity at a setting where the frequency of the maser is independent of the light intensity. This experiment is progressing extremely well and it has actually been possible, through light modulation, to use an electronic servo-tuning system to tune the maser cavity automatically. Preliminary results on this aspect of our work will be presented at the 27th Frequency Control Symposium in June. The other type of experiments, related closely to the cavity automatic tuning, consists in the study of the long term stability of the rubidium maser. This project is in its early stages and the results will be reported later on.

ANNEX B

LIGHT-SHIFT AND LIGHT-BROADENING IN THE Rb^{87} MASER

G. Busca, M. Têtu, J. Vanier

This paper has been accepted for publication in the Canadian Journal of Physics.

SUMMARY

A description of measurements of light-shift and light-broadening parameters for a Rb^{87} maser operating between the field independent levels is reported. A parallel study of the spectral profile of the D_1 pumping line is described. Comparison between the experimental results and theoretical calculations, taking into account the spatial inhomogeneity of the pumping light in the absorption cell is presented.

SOMMAIRE

On décrit des mesures de "light-shift" et de "light broadening" effectuées sur un maser opérant entre les niveaux indépendants du champ. Une étude parallèle du profil spectral de la raie de pompage D_1 est décrite. On compare les résultats expérimentaux aux résultats théoriques obtenus en tenant compte de l'inhomogénéité spatiale de la lumière de pompage dans la cellule d'absorption.

INTRODUCTION

Light-shift (L.S.) and light-broadening (L.B.) of atomic lines caused by optical pumping processes are well known phenomena. Various theoretical approaches (Barrat et al 1961, Happer et al 1967, Vanier 1969) and some experimental measurements either for passive (Arditi et al 1961, Alekseyev et al 1969) or for active devices (Davidovits et al 1966, Bazarov et al 1968) have been published. A rather complete summary of the knowledge on this subject up to 1971 is found in a review article by W. Happer (1972). Our interest on L.S. and L.B. comes from the study of the parameters wich are important for the frequency stability of the Rb^{87} maser. Short term stability of this maser has been reported recently somewhere else (Têtu et al 1972). In the present paper, the emphasis is placed first on studies related to the cavity tuning problem and secondly on the correlation between the spectral profile of the pumping light and the frequency shifts observed in the maser. The first study was accomplished in order to extract correct results for the L.S. and L.B. parameters. The second study allows a comparison between the theory and the experimental results. Our theoretical calculations show that the spatial inhomogeneity produced in the maser line by the inhomogeneous pumping rate, cannot be neglected. We have considered this phenomenon in some detail and show how it affects the maser operation.

2. THEORETICAL BACKGROUND

Expressions for the L.S. and L.B. could be derived following, for example, the theory of the optical pumping given by Vanier (1969). Taking into account the linearity of the L.S. and of the L.B. we may write (Bazarov et al, 1968).

$$\nu_\ell = \nu_o + \alpha I_{oo} \qquad (1)$$

and

$$\Delta\nu_\ell = \Delta\nu_o + \beta I_{oo} \quad , \qquad (2)$$

where ν_o and $\Delta\nu_o$ are respectively the rubidium frequency and the width of the hyperfine line without the effect of the light. The intensity of the incident light is represented by the expression:

$$I(\nu) = I_{oo} J(\nu) \quad , \qquad (3)$$

where I_{oo} is the peak value of this intensity and $J(\nu)$ is a spectral function normalized to a peak value of 1. The terms α and β are factors which depends on the spectrum $J(\nu)$ of the pumping light (see section 4). They represent respectively the shift (α) and the broadening (β) due to the light. From the equation of the linear cavity pulling of the frequency of a maser

$$\Delta\nu_m = \frac{Q_{\ell c}}{Q_\ell} \Delta\nu_c \qquad (4)$$

and eqs (1) and (2) we obtain

$$\nu_m \simeq \nu_o + \alpha I_{oo} + \Delta\nu_c \frac{Q_{\ell c}}{Q_{\ell o}} \left(1 + \frac{\beta I_{oo}}{\Delta\nu_o}\right) , \qquad (5)$$

where $Q_{\ell c}$ is the loaded cavity quality factor, $Q_{\ell o}$ is the line Q without the effect of the light and $\Delta\nu_c$ is the cavity frequency offset. In order to determine experimentally the value of α and β, the quantities ν_m, $\Delta\nu_c$ and I_{oo} must be measured directly on an operating maser and experiments must be made in which the maser frequency is determined as a function of the cavity pulling. For the measurement of α a cavity tuning technique for which $\Delta\nu_c = 0$ must be devised. For this tuning condition the maser frequency is independent of light broadening and depends only, in first approximation, on the L.S. In a more detailed analysis the frequency shift associated with spin-exchange must be considered.

From a practical point of view it is interesting to know the L.S. and the L.B. corresponding to 1% variation of the light intensity. We define these quantities as the relative L.S. and relative L.B. To relate these quantities to the parameters α and β it is only necessary to know the absolute value of I_{oo}.

3. EXPERIMENTAL RESULTS

3.1 Optical measurements

All the following measurements refer to the D_1 line spectrum. This spectrum was analysed on a Fabry-Perot interferometer in order to determine the shape, the shift and the peak value of the maximum intensity of the line as a function of the filter temperature. This was done in the following manner. The lamp-filter arrangement to be studied was placed directly in line with the Fabry-Perot interferometer. Another lamp, used as reference, was oriented at 90° to the axis of the interferometer. The lamps used were typically made of a one inch pyrex bulb filled with 2 Torr of Krypton and traces of Rb^{87}. The filter was a cylinder 3 inches in diameter and $1\frac{1}{2}$ inch long. A reflecting blade was placed on the axis of the interferometer and in the path of the two lamps. This blade was made to rotate slowly with the help of an intermittent motion gear which permitted to alternate the measurements between the two lamps while the interferometer was scanned. Details about the interferometer have been given by Missout et al, 1971). Fig. 1a and 1b give respectively the frequency displacement and the peak intensity of the pumping line as a function of the temperature of the filter cell. We can make the following observations on the results obtained:

a) At low filter temperatures, the presence of the partially removed $S_{\frac{1}{2}}$, $F = 2 \leftrightarrow P$ line of the adjacent order produces on the recording a displacement of the $S_{\frac{1}{2}}$, $F = 1 \leftrightarrow P$ line towards higher energies. Calculations show that the displacement δ, is given within approximations well realized in practice by the relation

$$\delta = + \frac{h_2}{h_1} (\nu_1 - \nu_2) \exp \frac{-(\nu_1 - \nu_2)^2}{(\Delta\nu_2)^2} \; 4 \ln 2 \,, \qquad (6)$$

where h, ν, $\Delta\nu$ are respectively the peak value, the center frequency and the full width of the gaussian line and indices 1 and 2 refer respectively to the $S_{\frac{1}{2}}$, $F = 1 \leftrightarrow P$ pumping line, and to the $S_{\frac{1}{2}}$, $F = 2 \leftrightarrow P$ line. Below a filter temperature T_F of 50°C, this apparent displacement is of the order of 50 MHz and decreases rapidly at higher temperatures (less than 10 MHz for $T_F = 70°C$). Values given on Fig. 1a have been corrected for this instrumental displacement, which otherwise would be interpreted wrongly as a true shift of the line.

b) In Fig. 1a interpolation of the experimental points is given approximatly by a straight line. This is related directly to the fact that the study is made on a small range of temperatures. Thus, experimentally, the optical displacement $\Delta\nu_{opt}$ turns out to be proportional to the Rb density. This is easily explained by the following considerations. Dis-

placement is caused by the unwanted absorption by the $S_{\frac{1}{2}}, F = 2 \leftrightarrow P$ line of the Rb^{85} vapor. Considering a filter of thickness ℓ and disregarding any effect of optical pumping inside the filter the following expression for the displacement is found

$$\Delta\nu_{opt} = \frac{(\Delta\nu_e)^2}{(\Delta\nu_a)^2} n(T_F)\, N_o . \ell\sigma_o(\nu_e - \nu_a) \exp \frac{-(\nu_e - \nu_a)^2}{\Delta\nu_a^2} 4 \ln 2 \quad (7)$$

or

$$\Delta\nu_{opt} = K\, n\, (T_F) , \quad (8)$$

where n is the density of Rb^{85} atoms. Index "e" refers to Rb^{87} pumping line and index "a" to the Rb^{85} absorption line. The calculation of Eq. 7 is given in the appendix. Deviations at higher temperatures from Eq. 8 is probably due to the effect of increased temperature gradients in the filter.

c) The spectral shape of the pumping line is well approximated by a gaussian shape with a width approximatly independent of the filter temperature.

All the results obtained refer to a non self-reversed lamp; a self-reversed lamp gives completely different results and an analysis of the data in this case is not practical.

3.2 Maser measurements

a) Measuring apparatus and cavity tuning techniques.

Cavity pulling and light-shifts were generally measured by beating the frequency of two Rb^{87} masers. The systems utilized were the same as those used for obtaining the frequency stability of the Rb^{87} maser (Têtu M., Busca G. and Vanier J., 1972). The use of one Rb^{87} maser as a reference allows very high resolution in the frequency measurement (fractional frequency deviation for an averaging time of 1 sec. is of the order of 10^{-13} and long term stability over 1 day is better than 4×10^{-11}). Light was varied either through an iris diaphragm or neutral density filters; the two methods gave the same results. Fine cavity tuning was accomplished through a small plunger at the bottom of the cavity. Criteria for tuning of the cavity are now considered. As mentioned previously (section 2), L.S. measurements involve the setting of the cavity at $\Delta\nu_c = 0$; the absolute error $\Delta\alpha$ on the α value due to an improper cavity tuning by $\Delta\nu_c$ is given by

$$\Delta\alpha = \frac{Q_{\ell c}}{Q_{\ell o}} \frac{\beta}{\Delta\nu_o} \Delta\nu_c \quad , \tag{9}$$

Usual criteria for cavity tuning cannot be used directly in this context. We have considered the following techniques: line Q modulation by Zeeman transitions broadening (Vanier, 1969) and maximum power output setting. The first technique, which is expected to be useful in long term stabilization of

the maser (Têtu et al, 1972), is not believed to be entirely appropriate for the present study. This is due to the fact that we have observed that the tuning condition depends slightly on the maser power output. Further studies are being made in order to understand this phenomenon. Consequently we have used the second method which dictates that the maser is tuned when maximum power is observed. In the use of this technique we have verified the independence of the cavity coupling on the fine cavity tuning and we have checked that the curve of the power output vs cavity tuning was symmetrical. To determine with high accuracy the cavity tuning at which the maser power is maximum, the frequency of the cavity is modulated at a low frequency (30 Hz) and synchronous detection of the output power is used through a lock in amplifier. The sensitivity of the method is better than 500 Hz. Alternatively an easier method consists in measuring the maximum in the d.c. output of an envelope detector when the cavity frequency is rapidly scanned; the error in this case is of the order of ~1 KHz.

b) Experimental results for the relative magnitude of the L.S. and L.B.

A typical example of cavity pulling measurements is shown in Fig. 2. These measurements refer to a cavity temperature of 59°C and a filter temperature of 73°C. The measurements were done either with D_1 , or with $D_1 + D_2$ lines. From Fig. 2

we see that a crossing point exists for all the straight lines representing the cavity pulling. At this point the maser frequency is independent of the light intensity. The amount of detuning required in order to obtain this condition is easily deduced from Eq. 5 and is given by

$$\Delta\nu_c = -\frac{Q_{\ell o}}{Q_{\ell c}} \Delta\nu_o \frac{\alpha}{\beta} \quad . \tag{10}$$

The fact that we obtain approximately the same crossing point by pumping either with $D_1 + D_2$ or D_1 lines implies that the $\frac{\alpha}{\beta}$ ratio is the same for $D_1 + D_2$ or D_1 lines.

In a latter experiment we have checked that at this crossing point the maser frequency was only slightly changed, when D_1 or $D_1 + D_2$ lines were used for pumping. The actual difference of $\simeq 4$ Hz shown in Fig. 5 was due to an uncontrolled systematic frequency shift that appeared between the two experiments.

These results are easily explained with the assumption that the effect of the D_2 line upon the maser oscillation is in first approximation negligible as supported by the following additional considerations: oscillation of our masers takes place by pumping with the D_1 line alone but not with the D_2 line alone; the D_2 line at the output of the isotopic filter contributes only for 30% of the total intensity; the cross section for the absorption of the D_2 line is twice as large as the

cross section for the D_1 line; this means that, at the center of the absorption cell, the intensity of the D_2 pumping line is greatly reduced compared to the intensity of the D_1 line, due to the absorption in the first few centimeters of this same cell. Measurements similar to those given in Fig. 2, analysed with the help of Eq. 5, as explained previously, allow the extraction of the parameter α and β. Fig. 3 gives the results obtained in a form which is immediately applicable to frequency stability considerations. This figure shows the L.S. and L.B. corresponding to a 1% variation of the incident light in operative condition.

L.S. measurements are shown in Fig. 4 for pumping with the D_1 line alone and for a temperature of 59°C. The extrapolated frequency at zero value of the light intensity is constant within 4×10^{-11}. This is of the order of the observed long term stability of the Rb^{87} maser. Possible error due to the tuning precision of ±1 KHz turned out to be ±0.05 Hz as calculated from Eq. 10. The data in Fig. 4 are plotted against the absolute I_{oo} value in order to make comparisons with the theoretical results (see section 4). To determine the absolute I_{oo} value for different filter temperatures measurements of the integrated flux of the D_1 line where performed through a calibrated solar cell. Knowing the spectral shape of the D_1 line from the recording obtained on the Fabry-Perot interferometer, the peak intensity I_{oo} was calculated.

The value of β is not easily measured for each filter temperature because the intensity of the D_1 line at the output of the interference filter was not sufficient at high filter temperatures to obtain a maximum in the power output. Thus, the range of light variation wich allows maser oscillation was very narrow. We found, however, approximatly the same value for β with excitation either with the D_1 or with the $D_1 + D_2$ lines at the intensity for which the measurements could be done. Fig. 3 gives the results for the relative L.B. when $D_1 + D_2$ lines are used at a cavity temperature of 59°C.

4. COMPUTER CALCULATIONS

A theoretical expression for the parameters α and β can be derived from previous work by Barrat et al (1961) and by Vanier (1969). In this analysis we neglect the small contribution of the tensor light-shift since the Zeeman L.S. and the light shift due to real transitions are ineffective (Mathur et al, 1968). From the results of these authors and after averaging over the doppler broadened distribution of the absorption line, we obtain the following expressions for the L.S. parameter

$$\alpha = \frac{\sigma_o}{2\pi^2} \int_{-\infty}^{+\infty} \int_{-\infty}^{+\infty} \frac{J(\nu)(\nu-\nu_a)}{(\nu-\nu_a)^2 + \left(\frac{\Delta\nu_a}{2}\right)^2} \exp - \frac{(\nu_a - \nu_o)^2}{(\Delta\nu_o)^2} \, 4 \ln 2 \, d\nu d\nu_a \,, \tag{11}$$

where ν_a is the line center frequency of a given class of atoms, ν_o is the line center frequency of the doppler broadened line, $\Delta\nu_a$ is the natural line width, $\Delta\nu_o$ the doppler width and σ_o the absorption cross section. A similar expression can be derived for the L.B. parameter β

$$\beta = \frac{\sigma_o}{2\pi} \int_{-\infty}^{+\infty} J(\nu) \exp - \frac{(\nu - \nu_a)^2}{(\Delta\nu_o)^2} \quad 4 \ln 2 \, d\nu \, . \qquad (12)$$

β is related to the pumping rate defined by the expression

$$\beta I_{oo} = \frac{\Gamma}{2\pi} \, . \qquad (13)$$

In the case of the Rb maser, where $I(\nu)$ is a function of the coordinates in the storage bulb, these integral can be evaluated only in a numerical way. L.S. and L.B. are functions of the position into the absorption cell and inhomogenous broadening of the maser line takes place. In fact, the buffer gas inhibits practically all movement of the Rb atoms. This situation is quite different from that encountered in the H maser where atoms move freely and average out the spatial inhomogeneity of the r.f. field. Calculations related to the inhomogenous pumping rate Γ have been published (Tessier et al, 1971). The present paper extends the calculation to the light shift parameter. Considering cylindrical coordinates and taking the origin of z at the top of the cavity and the light propagation in the di-

rection of z the power emitted by the atoms in the element dV at position (z, r) has the spectral shape given by (Tessier et al, 1971, Vanier 1971).

$$dP = nh\nu dV \frac{2\beta^2 \Gamma A}{\gamma_1(\frac{1}{2}\Gamma + \gamma_2) + \left[\gamma_1/(\frac{1}{2}\Gamma + \gamma_2)\right](\omega-\omega')^2 + (1-\Gamma B)4\beta^2} , \tag{14}$$

where $\omega' = 2\pi(\nu_o + \alpha I_{oo})$. To determine $P(z, r)$ one must know the function $\Gamma(z, r)$ and $\omega' = \omega'(z, r)$. By integrating expression 14 over the cavity volume one obtains the spectral power distribution of the inhomogeneously, broadened line. Maser oscillation takes place at the frequency where maximum gain is obtained.

The determination of Γ and ω' requires the knowledge of the spectral distribution of $I(\nu, z, r) = I_{oo}J(\nu, z, r)$. We assume for $z = 0$ a spectral distribution independent of r

$$J(\nu, o, r) = \exp \frac{-(\nu - \nu_e)^2}{(\Delta\nu_e)^2} \, 4 \ln 2 \quad . \tag{15}$$

The pumping rate Γ_o at $z = 0$ is easily calculated from Eq. 13

$$\Gamma = \int_{-\infty}^{+\infty} I(\nu)\sigma(\nu)\, d\nu \quad . \tag{16}$$

The light shift is calculated form Eq. 11. The law of attenuation of the light is (Tessier et al, 1971)

$$dI(\nu, z, r) = -n(z, r)\, \sigma(\nu)\, I(\nu, z, r)dz \quad , \tag{17}$$

where $n(z, r)$ is the number of atoms per unit volume wich absorb the pumping light and is expressed by

$$n(z, r) = \frac{3n_o\gamma_1}{5\Gamma + 8\gamma_1} + \frac{8n_o}{5\Gamma + 8\gamma_1} \cdot \frac{2\beta\Gamma A}{\left[\gamma_1/\left(\tfrac{1}{2}\Gamma + \gamma_1\right)\right](\omega - \omega')^2 + \left(1 - \Gamma B\right)4\beta^2} \quad . \tag{18}$$

In first approximation we can neglect the second term in Eq. 18. In fact, its contribution is small. $I(\nu, z, r)$ and Γ in this case are independent of r. From a knowledge of Γ_o, $I(\nu, z)$ can be evaluated by the following iterative method. The cell is divided vertically in N layers; within each layer, Γ and n are considered to be constant. For the 1st layer one takes the value Γ_o for $\Gamma(z)$ and from Eq. 18 one calculates n. Using Eq. 17 one computes the spectral profile of the exictation at the exit of the 1st layer and this determines a new Γ and ω'. This new value of Γ is used to calculate "n" for the second layer and so on. Fig. 5 gives one example of the computer calculation for the light shift (αI_{oo}) and Γ vs z; the spectral profile of the pumping light is shown in Fig. 6. Values of typical parameters which have been used are given in table 1.

TABLE 1

Physical parameters used to calculate Γ and ω'

σ_o	$= 2.10^{11}$ cm^2	$\Delta\nu_a$	= 500 MHz
$\nu_e - \nu_a$	= 300 MHz	Γ_o	= 1000
$\Delta\nu_e$	= 1000 MHz	N	= 20

On the one hand, the light shift tends to increase with Z because the displacement and asymmetry of the pumping line increase with Z . On the other hand, the light shift tends to decrease with Z because the peak value of I_{oo} decreases with Z . One observes that if there exist a non coincidence between the pumping line maximum and the absorption line maximum, the displacement and asymmetry increases with Z very rapidly until a saturation limit is reached. Thus, the actual spectrum responsible for the observed light shift (spectrum near the center of the cavity) is very different from that shown at $z = 0$. For this reason, theories wich do not take into account the spatial inhomogeneity of the pumping light (Davidovits et al, 1966, Alekseyev et al, 1970) represent a crude approximation of the physical situation.

All the parameters of Eq. 14 being known, the integration over the cavity volume can be performed. One obtains the spectral power distribution and in particular the frequency of oscillation, the width and symmetry properties of the hyperfine line. By varying the light incident on the cell (I_{oo} value) for a given spectral distribution (determined by the isotopic filter temperature), different oscillation frequencies and line width are obtained. Figure 7 give these results. One example of the asymmetry of the line is also given · The values α and β are the slopes of the curves shown in Fig. 7. These slopes are not constant over the whole range of I_{oo} values.

The following comments can be added in relation to the above calculations:

a) even if the L.S. is a rapidly varying function of Z the region near the center of the cavity determines the oscillation frequency. In fact, integration of Eq. 14 is roughly equivalent to averaging the contribution of each layer by a function like $\sin^2 \pi \frac{z}{\ell}$. This is due to the form of the r.f. field whose configuration is controlled by the mode used in the cavity, which in our case is TE 021.

b) Deviations of the light shift vs light intensity from a straight line are visible in fig. 7 . Unfortunatly this was not observed experimentally because the maser oscillates only in a narrow range of light intensity.

c) As shown on fig. 7 the asymmetry in the hyperfine line profile is evident but not too important.

5. COMPARISON OF THE CALCULATIONS WITH EXPERIMENTAL RESULTS

The experimental values of I_{oo} range from 50×10^3 to $200 \times 10^3 \frac{\text{phot}}{\text{cm}^2 \text{sec. Hz}}$. These limits were also evaluated from a direct measurement of the pumping rates on the maser through the method described by Vanier (1968). Calculated relative values of α and β agree well with the experimental values. However the calculated absolute values are only in the correct order of magnitude and a normalization of the theoretical values must be made in order to obtain agreement with the experimental

data. The experimental values for α and β, deduced from the results given in Fig. 3 and 4, for a cavity temperature of 59°C are shown in Fig. 8. In the case of the parameter β we make the assumption that the effect of the D_2 line was negligible. The theoretical values of α and β are shown in Fig. 8. They are the slopes of the curves given in Fig. 7, the slopes being measured within the actual range of I_{oo} values. In this range the slopes are approximatly constant. Typically, for $I_{oo} = 100 \times 10^3$ and $\nu_e - \nu_a = 200$ MHz the experimental L.S. is ~5 Hz compared to a calculated value of 15 Hz and the calculated absolute value of β is greather than the experimental value by a factor of 2.

6. CONCLUSION

L.S. and L.B. in the Rb^{87} maser have been measured in operative conditions. The experimental values of α and β have been compared with the calculated values. The agreement is found to be only satisfactory. Computer calculations show that the maser line is slightly inhomogeneously broadened. These calculations also show that the L.S. and the L.B. are linear functions of the light intensity in the actual range of operation of the maser.

The results obtained give useful information about the influence of the light intensity on the frequency stability of the maser and can also be used for the actual design of a maser with improved frequency stability. This is because, one can

choose between various criteria for the cavity tuning. In particular the frequency of the maser could be made independent of the light intensity by a proper tuning of the cavity.

ACKNOWLEDGMENT

We would like to thank the National Research Council of Canada, the National Aeronautics and Space Administration and the Department of Education of the Province of Quebec for their financial help through the course of this work .

We would like also to thank Mr. C. Prince for his competent help in building many of the electronic circuits used in the measurements described in this paper.

BIBLIOGRAPHY

ALEKSEYEV E.I. and BAZAROV Y.E.N., 1970, Radio Eng. and Electron. Phys. 15, 851.

ALEKSEYEV E.I., BAZAROV Y.E.N. and LEVSHIN A.E., 1969, Radioteknika i Elektronika, 14, 11, 2026 (Radio Eng. and Electron. Phys. 14, 11, 1750).

ARDITI M. and CARVER T.R., 1961, Phys. Rev. 124, 800-809.

BARRAT J.P. and COHEN-TANNOUDJI C., 1961, J. Phys. Radium 22, 329, 443.

BAZAROV Y.E.N. and GUBIN V.P., 1968, Radioteknika i Elektronika, 13, 1519 (Radio Eng. and Electron., Phys. 13, 1324).

DAVIDOVITS P. and NOVICK R., 1966, Proc. IEEE, 54, 155.

HAPPER W., 1972, Rev. Mod. Phys. 44, 169.

HAPPER W. and MATHUR B.S., 1967, Phys. Rev. 163, 12.

MATHUR B.S., TANG H. and HAPPER W., 1968, Phys. Rev. 171, 11.

MISSOUT G., VAILLANCOURT R., TETU M. et VANIER J., 1971, Rev. Phys. Appl. 66, 307.

TESSIER M. et VANIER J., 1971, Can. Phys. 49, 2680.

TETU M., BUSCA G. et VANIER J., 1972, Proceedings of the Twenty-sixth annual frequency control symposium.

VANIER J., 1969, Can. J. Phys. 47, 1461.

VANIER J., 1969, Patent No. 3, 435, 369.

VANIER J., 1968, Phys. Rev. 168, 129.

VANIER J., 1971, Basic Theory of Lasers and Masers, Gordon and Breach Science Publishers, N.Y.

FIGURES CAPTIONS

1) a) Shift of the D_1 line versus filter temperatures.

   b) Intensity of the D_1 line versus filter temperatures.

2) Typical cavity pulling measurements.

3) Relative L.S. and L.B. versus filter temperatures.

4) Light-shift measurements in the case of the D_1 pumping line.

5) Calculated light-shift and pumping rate Γ versus the penetration depth in the absorption cell.

6) Calculated spectral behaviour of the pumping line at different penetration depths.

7) Calculated maser light-shift and line width versus light intensity. A typical example of the calculated inhomogeneous hyperfine line.

8) Comparison between the experimental and calculated values of the α and β parameters.

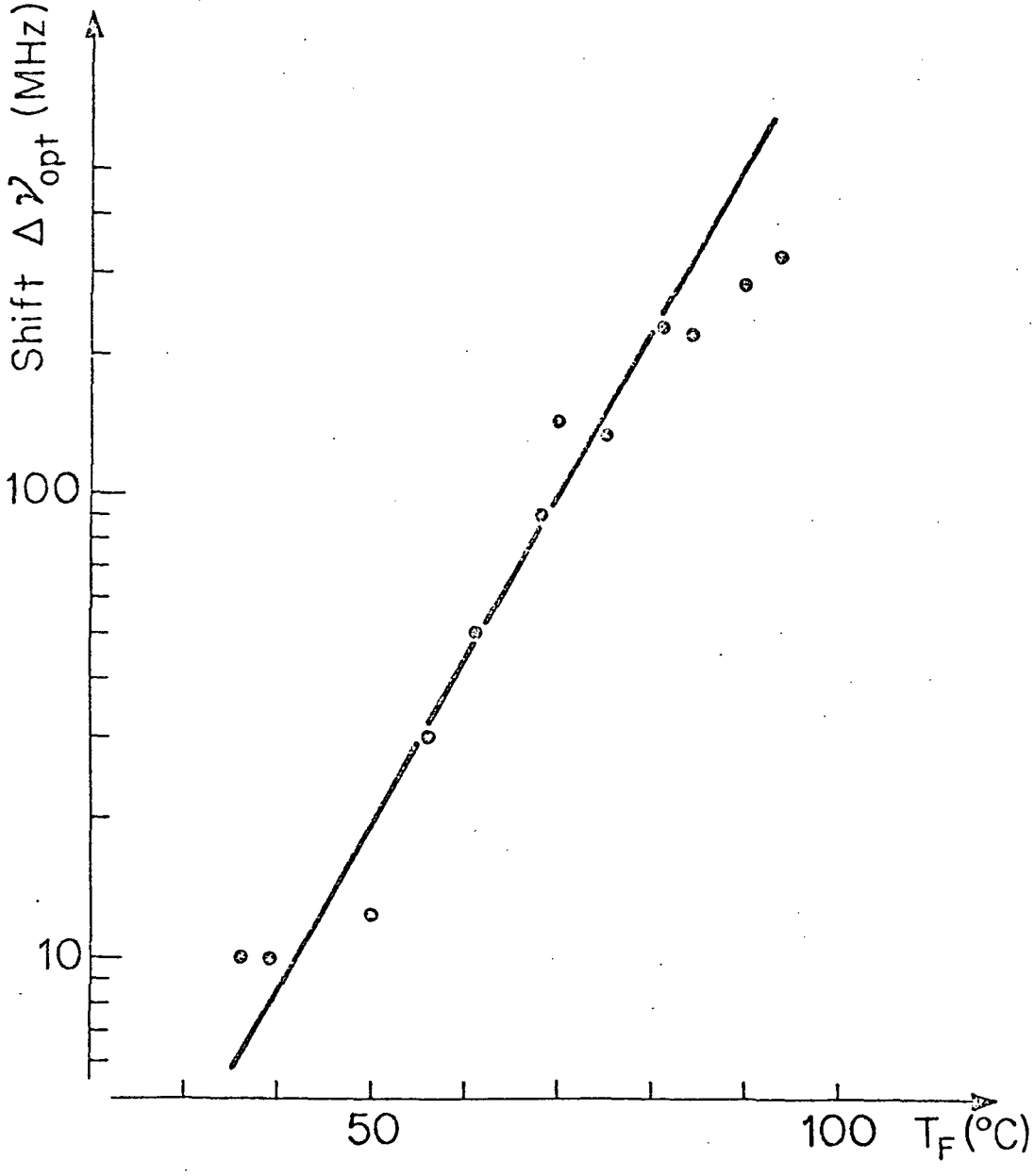

Figure 1a

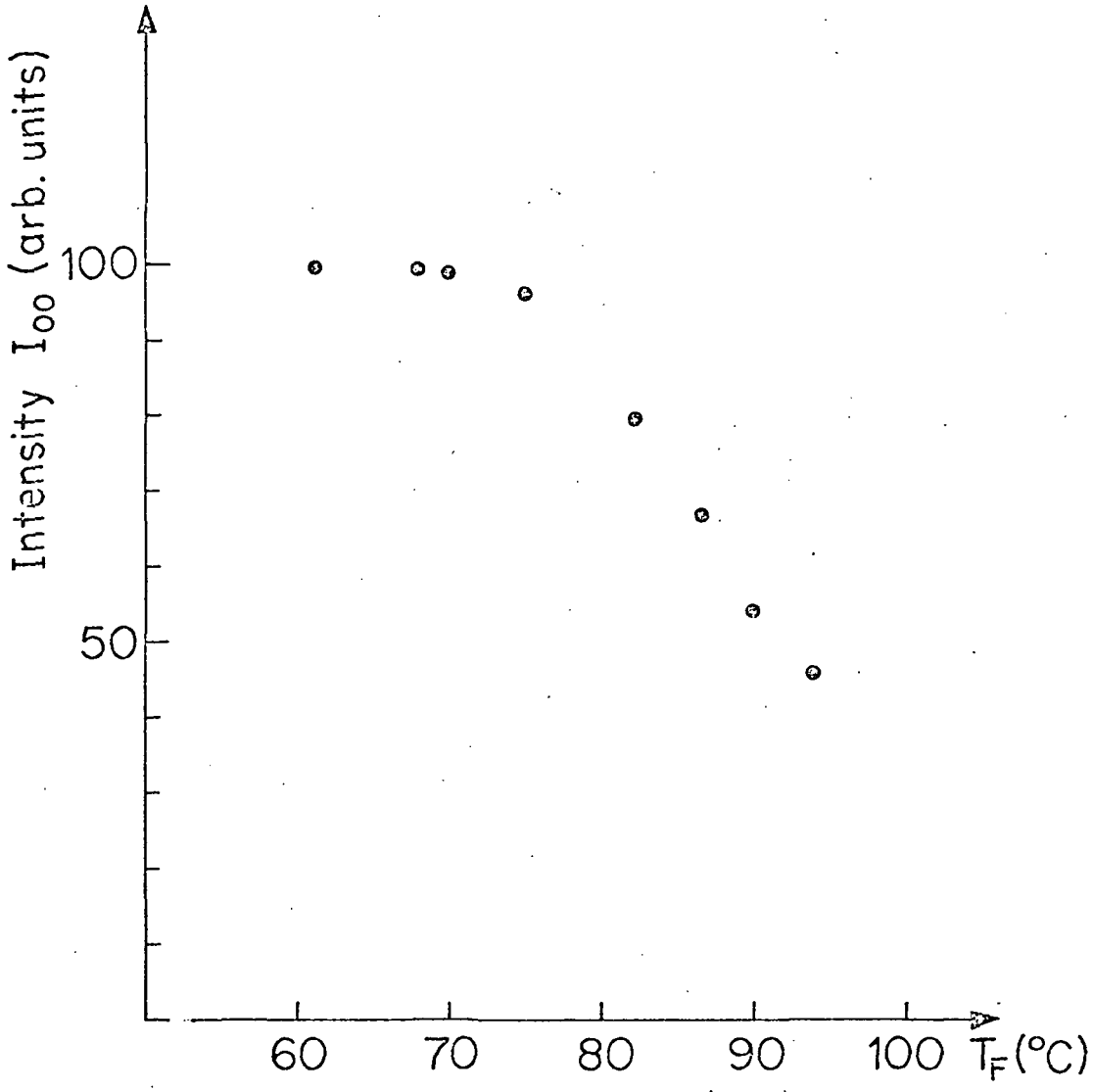

Figure 1b

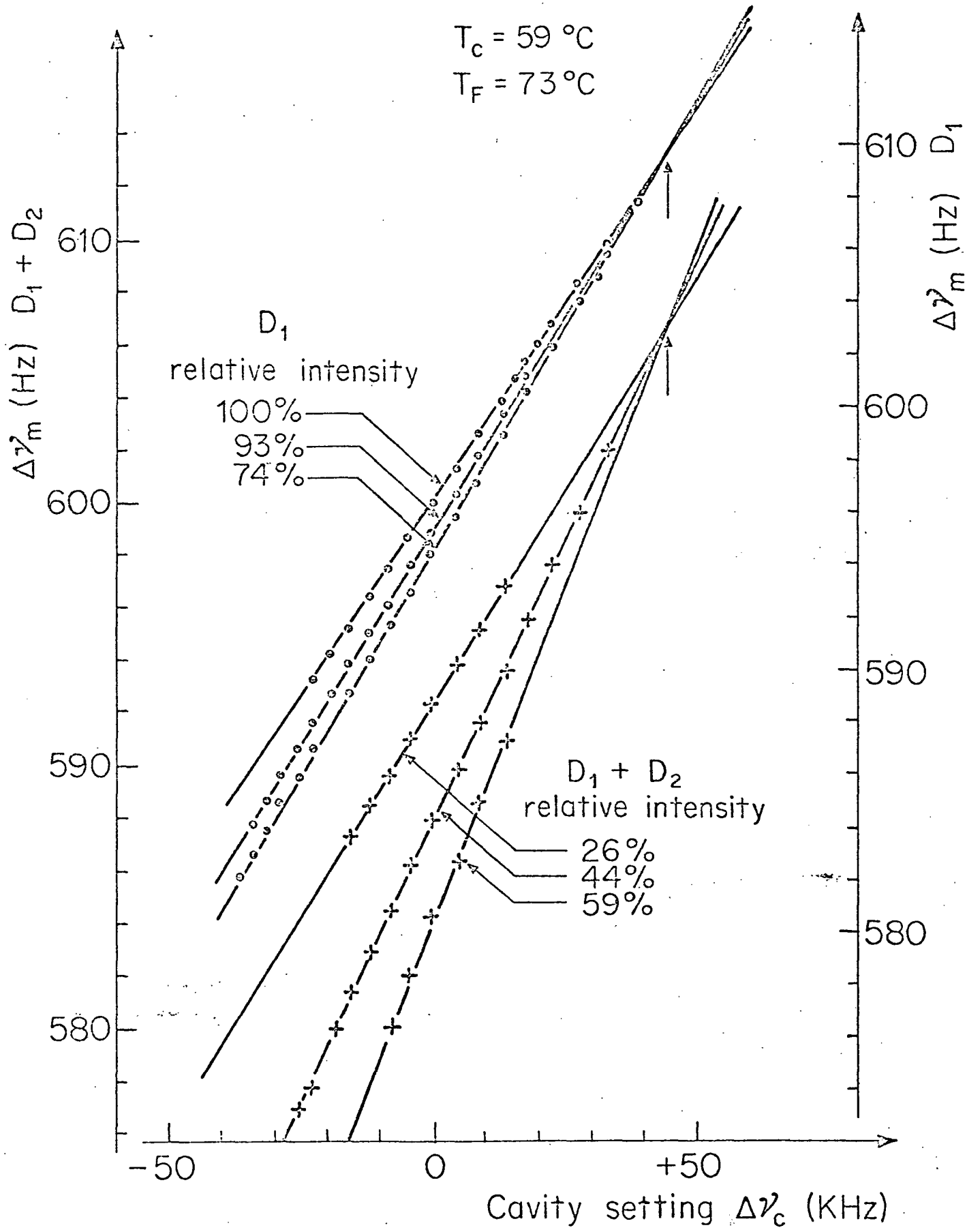
T_c = 59 °C
T_F = 73 °C
$\Delta\nu_m$ (Hz) $D_1 + D_2$
$\Delta\nu_m$ (Hz) D_1
610
600
590
580
610
600
590
580
D_1
relative intensity
100%
93%
74%
$D_1 + D_2$
relative intensity
26%
44%
59%
−50
0
+50
Cavity setting $\Delta\nu_c$ (KHz)

Figure 2

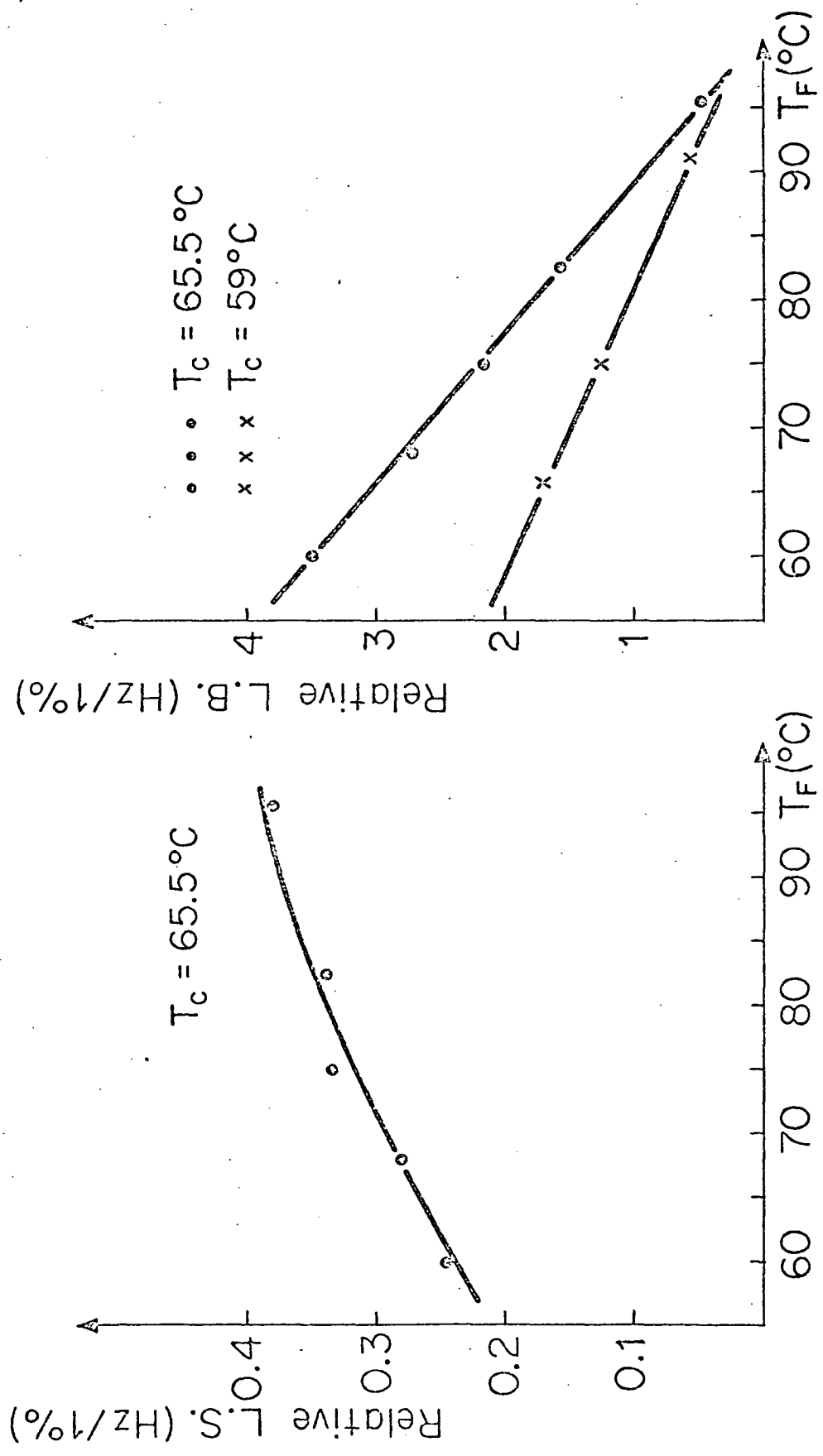
Relative L.S. (Hz/1%)
0.4
0.3
0.2
0.1
T_c = 65.5°C
60
70
80
90 T_F(°C)
Relative L.B. (Hz/1%)
4
3
2
1
• • • T_c = 65.5 °C
x x x T_c = 59°C
60
70
80
90 T_F(°C)

Figure 3

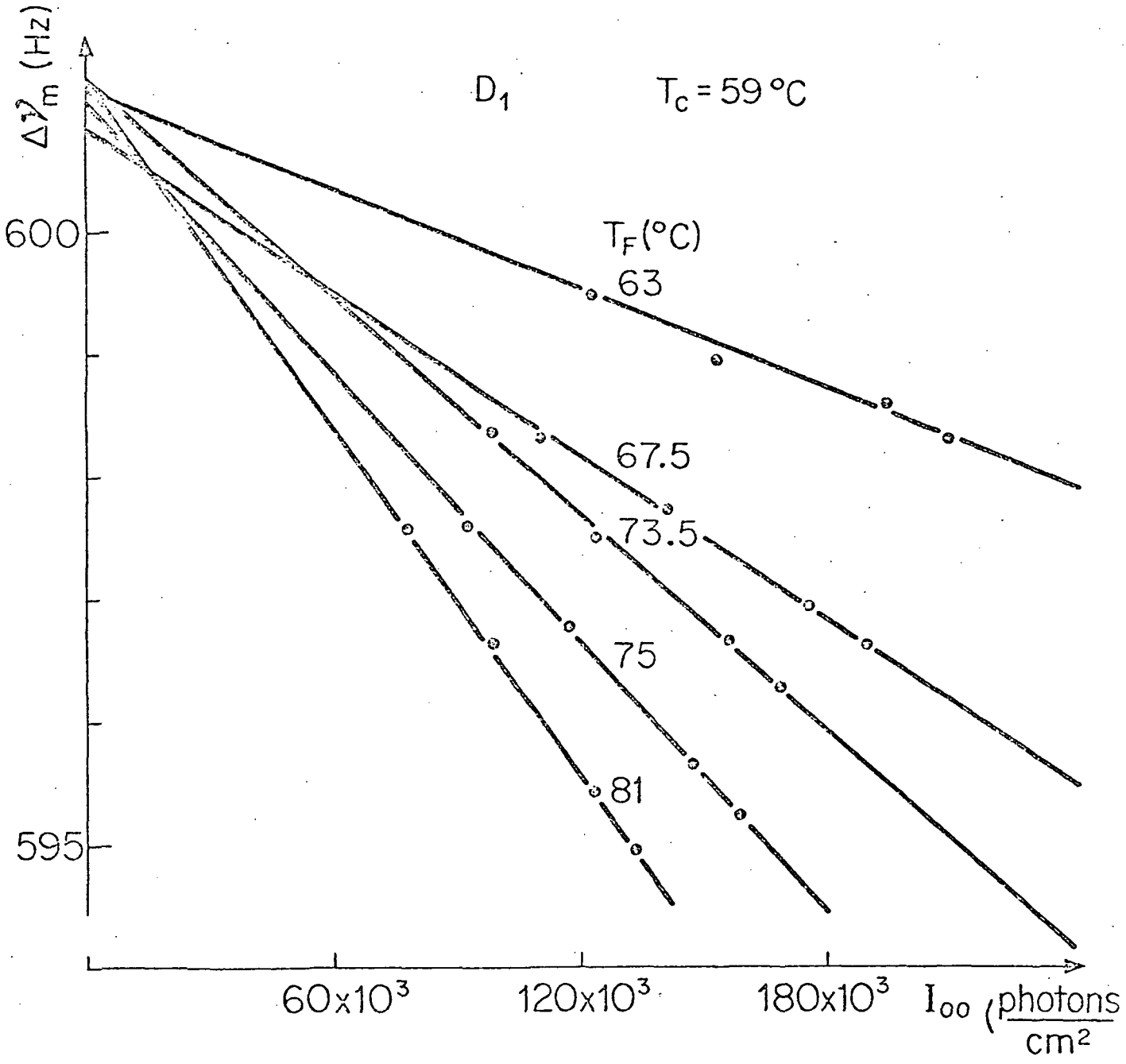
$\Delta\nu_m$ (Hz)
D_1
$T_c = 59\,°C$
T_F(°C)
63
67.5
73.5
75
81
600
595
60×10^3
120×10^3
180×10^3
I_{oo} (photons/cm²)

Figure 4

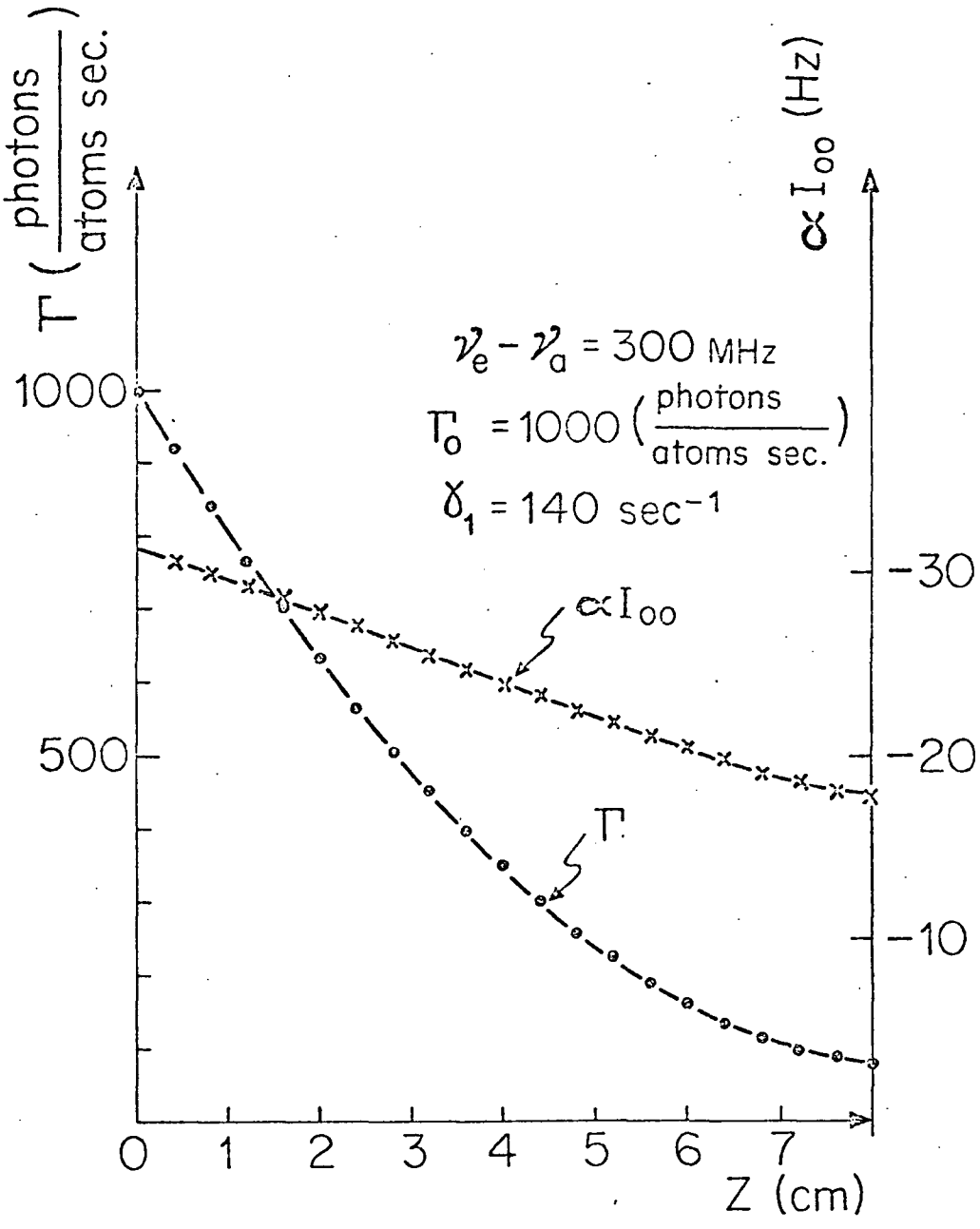
Γ (photons / atoms sec.)
∝ I₀₀ (Hz)
$\nu_e - \nu_a$ = 300 MHz
Γ_0 = 1000 (photons / atoms sec.)
γ_1 = 140 sec⁻¹
1000
500
-30
-20
-10
∝ I₀₀
Γ
0
1
2
3
4
5
6
7
Z (cm)

Figure 5

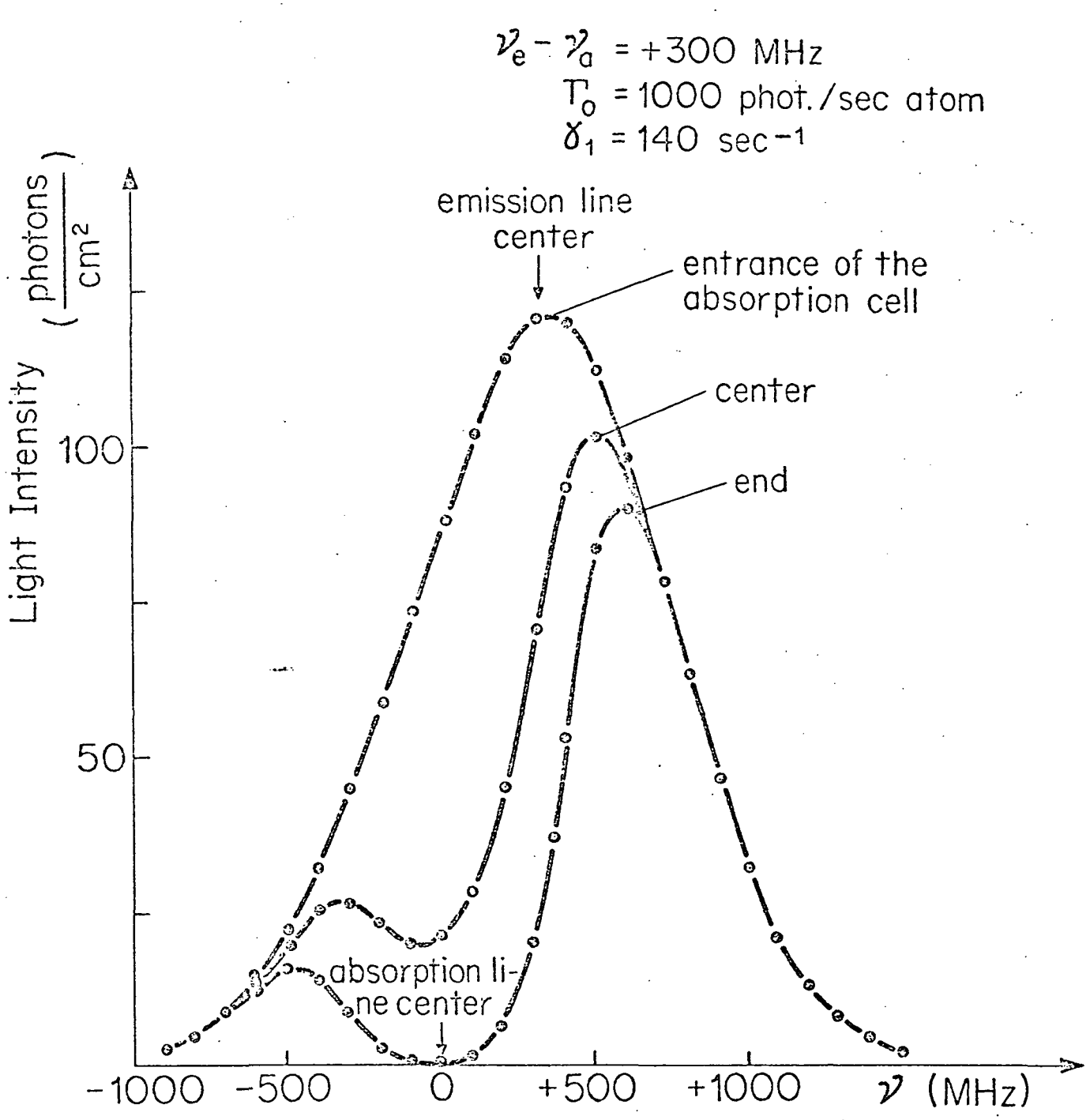
$\nu_e - \nu_a = +300$ MHz
$T_0 = 1000$ phot./sec atom
$\gamma_1 = 140$ sec^{-1}
Light Intensity ($\frac{\text{photons}}{\text{cm}^2}$)
100
50
emission line center
entrance of the absorption cell
center
end
absorption line center
-1000
-500
0
+500
+1000
ν (MHz)

Figure 6

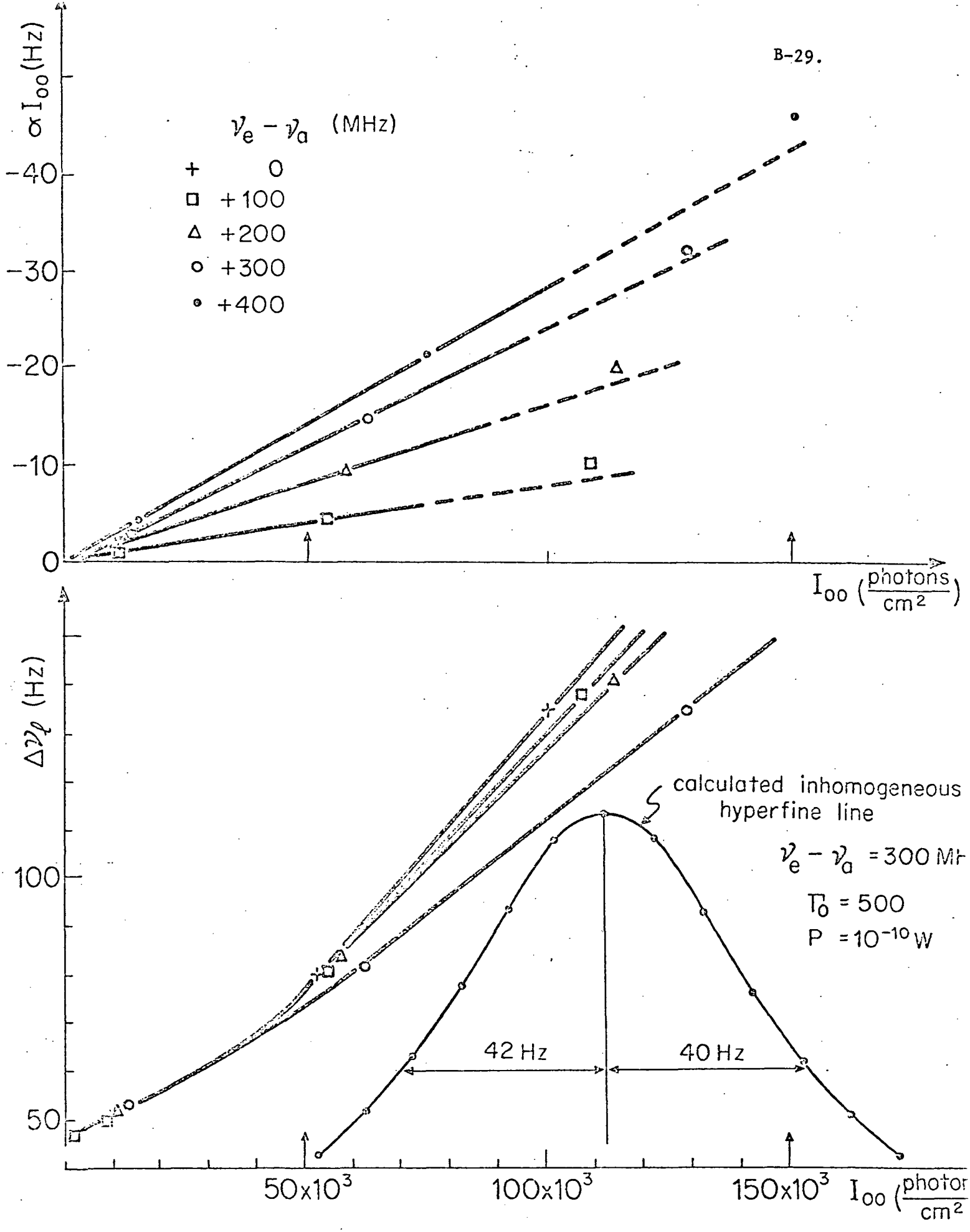
$\propto I_{oo}$(Hz)
$\nu_e - \nu_a$ (MHz)
+ 0
□ +100
△ +200
○ +300
⊙ +400
-40
-30
-20
-10
0
I_{oo} ($\frac{photons}{cm^2}$)
$\Delta\nu_\ell$ (Hz)
100
50
calculated inhomogeneous hyperfine line
$\nu_e - \nu_a$ = 300 MH
Γ_0 = 500
P = 10^{-10} W
42 Hz
40 Hz
50×10^3
100×10^3
150×10^3
I_{oo} (photon
cm^2

Figure 7

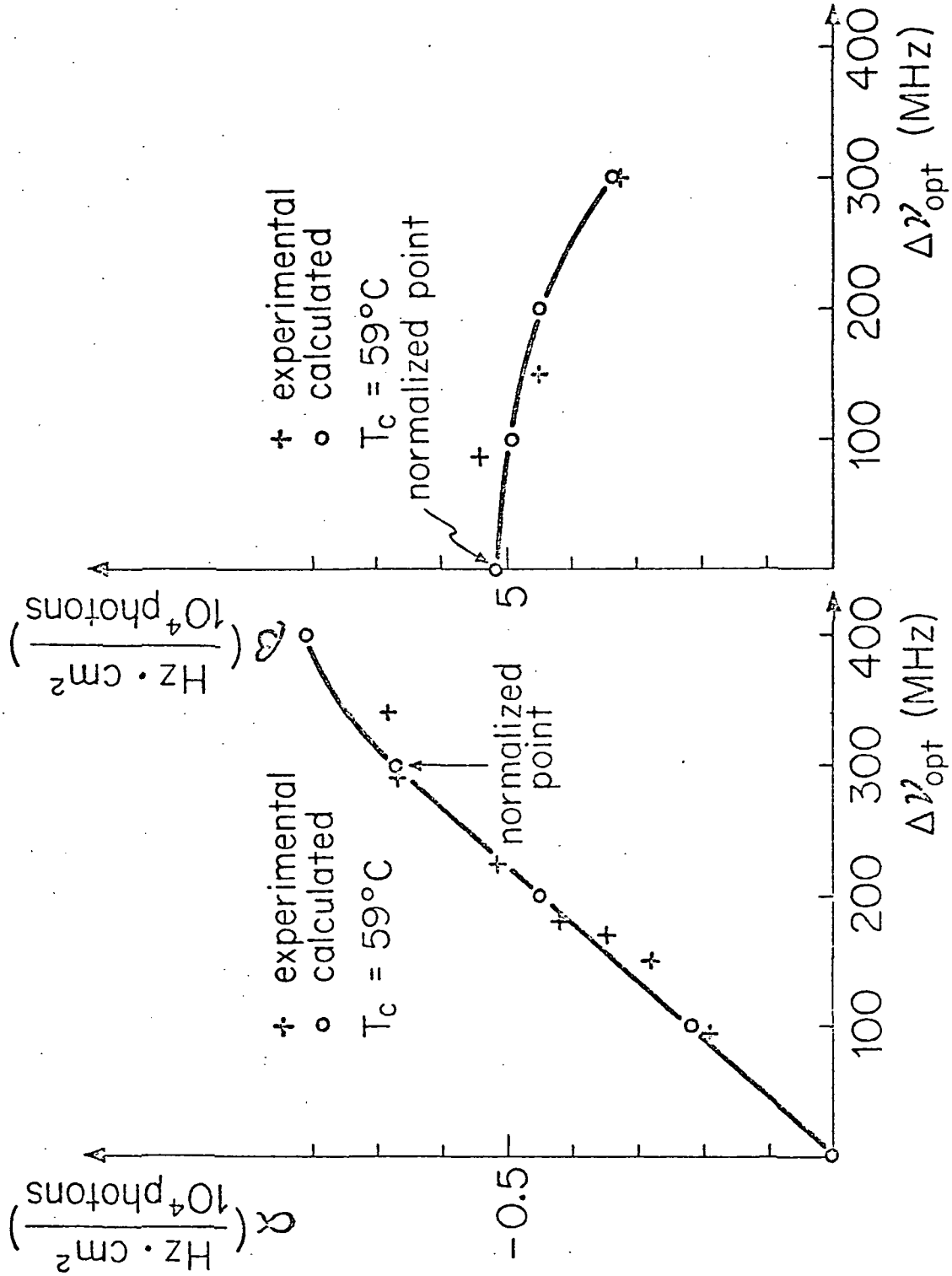
α (Hz · cm² / 10⁴ photons)
-0.5
5
+ experimental
o calculated
Tc = 59°C
normalized point
100 200 300 400
Δν opt (MHz)

Figure 8

APPENDIX

We suppose that the pumping line incident on the isotopic filter has a gaussian shape given by

$$I(\nu) = I_o \exp \frac{-(\nu - \nu_e)^2}{\Delta\nu_e^2} 4 \ln 2 \quad . \tag{1}$$

Taking the light propagation in the direction of Z. the attenuation law is

$$dI(\nu, Z + dZ) = -I(\nu, Z)\, n\sigma(\nu) Z.dZ \quad , \tag{2}$$

where $\sigma(\nu)$ is the cross section for absorption and n is the density of the Rb^{85} atoms. We suppose that $\sigma(\nu)$ has a gaussian shape given by

$$\sigma(\nu) = \sigma_o \exp \frac{-(\nu - \nu_a)^2}{\Delta\nu_a^2} 4 \ln 2 \quad . \tag{3}$$

Assuming n independent of Z Eq. 2 is readily integrated and yields

$$I(\nu, Z) = I_o \exp\left[- \frac{(\nu-\nu_e)^2}{\Delta\nu_e^2} 4 \ln 2 - nZ\, \sigma_o \exp - \frac{(\nu-\nu_a)^2}{\Delta\nu_a^2} 4 \ln 2 \right] . \tag{4}$$

The previous hypothesis means that we neglect the possible effect of the optical pumping inside the filter.

We want to obtain the frequency ν_m of the maximum of $I(\nu, \ell)$, ℓ being the filter thickness.

By derivation of Eq. 5 we obtain for ν_m

$$\frac{(\nu_m - \nu_e)}{\Delta\nu_e^2} - nZ\,\sigma_o\,\frac{\nu_m - \nu_a}{\Delta\nu_a^2}\exp - \frac{(\nu_m - \nu_a)^2}{\Delta\nu_a^2}\,4\ln 2 = 0\,. \quad (5)$$

We write for ν_m the expression

$$\nu_m = \nu_e + \Delta\nu_{opt}\,. \quad (6)$$

Solution of Eq. 5 is done with the approximation that the displacement $\Delta\nu_{opt}$ is negligible compared to $\nu_e - \nu_a$. This approximation corresponds to the actual experimental situation. From Eq. 5 one obtains

$$\Delta\nu_{opt} = \left(\frac{\Delta\nu_e}{\Delta\nu_a}\right)^2 n(T_F)\ell\sigma_o\,(\nu_e - \nu_a)\exp\frac{-(\nu_e - \nu_a)^2}{\Delta\nu_a^2}\,4\ln 2\,,$$

which is Eq. 7 of section 3.1.

ANNEX C

CAVITY TUNING AND LIGHT-SHIFT IN THE Rb^{87} MASER

G. Busca, M. Têtu and J. Vanier

This paper will be presented at the 27th Frequency Control Symposium in June 1973 at Atlantic City.

CAVITY TUNING AND LIGHT-SHIFT IN THE Rb^{87} MASER

G. BUSCA, M. TETU and J. VANIER

Laboratoire d'Electronique Quantique
Département de Génie électrique
Université Laval, Québec 10, CANADA

A new method for automatic cavity tuning of the Rb^{87} maser is proposed.

The following theoretical relationship accounting for the light-shift, cavity pulling and spin-exchange phenomena is deduced :

$$\nu_m = \nu_0 + \alpha I_{00} + \frac{2Q_{\ell c}}{\nu_0} \Delta\nu_c - C \frac{\Delta\nu_0 + \beta I_{00}}{2} \qquad (1)$$

where ν_m is the maser output frequency, ν_0 and $\Delta\nu_0$ are respectively the rubidium frequency and the width of the hyperfine line without the effect of the light, $Q_{\ell c}$ is the loaded cavity quality factor, C is a constant related to spin-exchange shift, $\Delta\nu_c$ is the cavity offset, α and β are factors depending on the normalized pumping line shape and I_{00} is the peak value of the line. The factors α and β represent respectively the light-shift and the light-broadening of the atomic energy levels due to the pumping light. Equation (1) shows the existence of a cavity setting for which the maser frequency is independent of the light intensity (named here Light Independent Frequency Setting). To obtain a LIFS, the cavity must be detuned by an amount $\Delta\nu_c$ given by :

$$\frac{2Q_{\ell c}}{\nu_0} \Delta\nu_c - C = -\frac{2\alpha}{\beta} \qquad (2)$$

In order to obtain sufficiently good short term stability at the LIFS, $\Delta\nu_c$ must be kept at a minimum value. This corresponds to a minimum isotopic filter temperature which is a requirement opposite to the optimum filter efficiency condition. In our case, a good compromise is obtained experimentally for an isotopic filter temperature of $64^{\circ}C$ and cavity temperature of $68^{\circ}C$. The output power at the LIFS is a few percent below the maximum output power. The experimental results obtained are in good agreement with equation (1). At the LIFS, the maser frequency variations are contained within 5×10^{-12} over the whole range of the light intensity. The previous results allow to use the LIFS as a method for an automatic cavity tuning, in which the parameter to be varied is the light-intensity and the error signal is the maser frequency variation.

The great advantage of the LIFS technique is the independence of the maser frequency from the light intensity. Some preliminary results obtained by using a closed loop feedback electronic system for tuning the cavity are presented.